Coupled Systems Mechanics, *Vol. 6, No. 2 (2017) 207-227*
DOI: https://doi.org/10.12989/csm.2017.6.2.207

Thermo-mechanical analysis of carbon nanotube-reinforced composite sandwich beams

Farzad Ebrahimi* and Navid Farazamandnia

Department of Mechanical Engineering, Faculty of Engineering, Imam Khomeini International University, Qazvin, P.O.B. 16818-34149, Iran

(Received October 27, 2016, Revised April 18, 2017, Accepted May 11, 2017)

Abstract. In this paper Timoshenko beam theory is employed to investigate the vibration characteristics of functionally graded carbon nanotube-reinforced composite (FG-CNTRC) Beams with a stiff core in thermal environment. The material characteristic of carbon nanotubes (CNT) are supposed to change in the thickness direction in a functionally graded form. They can also be calculated through a micromechanical model where the CNT efficiency parameter is determined by matching the elastic modulus of CNTRCs calculated from the rule of mixture with those gained from the molecular dynamics simulations. The differential transform method (DTM) which is established upon the Taylor series expansion is one of the effective mathematical techniques employed to the differential governing equations of sandwich beams. Effects of carbon nanotube volume fraction, slenderness ratio, core-to-face sheet thickness ratio, different thermal environment and various boundary conditions on the free vibration characteristics of FG-CNTRC sandwich beams are studied. It is observed that vibration response of FG-CNTRC sandwich beams is prominently influenced by these parameters.

Keywords: functionally graded carbon nanotube-reinforced composite; thermo-mechanical vibration; Hamilton's principle

1. Introduction

The need for high performance and low weight structures makes sandwich construction one of the best choices in aircrafts, space vehicles and transportation systems. Functionally graded materials (FGMs) are composite materials with inhomogeneous micromechanical structure in which the material properties change smoothly between two surfaces and leads to a novel structure which can withstand large mechanical loadings in high temperature environments (Ebrahimi and Salari 2015). Presenting novel properties, FGMs have also attracted intensive research interests, which were mainly focused on their static, dynamic and vibration characteristics (Ebrahimi and Rastgoo, 2008a, b, c, Ebrahimi 2013, Ebrahimi *et al.* 2008, 2009a, b, 2016a, Ebrahimi and Zia 2015, Ebrahimi and Mokhtari 2015, Ebrahimi and Salari 2015a, b, Tounsi *et al.* 2016).

Also many researches have been conducted on vibration, buckling and post-buckling analysis of

*Corresponding author, Ph.D., E-mail: febrahimy@eng.ikiu.ac.ir

http://www.techno-press.org/?journal=csm&subpage=8 ISSN: 2234-2184 (Print), 2234-2192 (Online)

sandwich structures with FGM face sheets (Zenkour 2005, Bhangale and Ganesan 2006, Pradhan and Murmu 2009, Anandrao *et al.* 2010, Zenkour and Sobhy 2010, Fekrar *et al.* 2012, Saidi *et al.* 2013, Hamidi *et al.* 2015). Actually, material gradation will reduce maximum stresses and change the spatial location where such maximums arise (Rahmani and Pedram 2014). This provides the opportunity of fitting material variation to attain desired stresses in a structure. Also many other researchers investigated the vibration bending and buckling of nanostructures Ebrahimi and Salari 2015a, b, 2016, Ebrahimi *et al.* 2015a, 2016c, Ebrahimi and Nasirzadeh 2015, Ebrahimi and Barati 2016a, b, c, d, e, f, Ebrahimi and Hosseini 2016 a, b, c).

On the other hand, the thermo-mechanical effect on FG structures is studied by many researchers. Tounsi *et al.* (2013) presented a refined trigonometric shear deformation theory for thermoelastic FG sandwich plates (Tounsi *et al.* 2013). Most recently Ebrahimi and Barati (2016g, h, i, j, k, l, m, n, o, p, q, r, s, t, u, v, 2017a, b) and Ebrahimi *et al.* (2017) explored thermal and hygro-thermal effects on nonlocal behavior of FG nanobeams and nanoplates. Carbon nanotubes have extraordinary mechanical properties. Due to their outstanding properties such as, superior mechanical, electrical, and thermal nanotubes have attracted growing interest and are considered to be the most promising materials for applications in nanoengineering (Lau and Hui 2002, Lau *et al.* 2004, Esawi and Farag 2007). So many applications for carbon nanotubes have been proposed by researchers: conductive polymers; energy conversion devices and energy storage; sensors; field emission displays; replacing silicon in microcircuits; multilevel chips; probes for SPM (scanning probe microscopy) (Esawi and Farag 2007). The CNT-based nanocomposite devices may withstand high temperature during manufacture and operation. Various studies show that the physical property of carbon nanotubes depends on temperature, from which we believe that the elastic constants of nanotubes, such as Young's modulus and shear modulus, are also temperature dependent (Fidelus *et al.* 2005, Bonnet *et al.* 2007). However, it is remarkably difficult to directly measure the mechanical properties of individual SWCNTs experimentally due to their extremely small size.

In 1994 Ajayan *et al.* (Ajayan *et al.* 1994) studied the polymer composites reinforced by aligned CNT arrays. Since then, many researchers inspected the material properties of CNTRCs (Odegard *et al.* 2003, Thostenson and Chou 2003, Griebel and Hamaekers 2004, Hu *et al.* 2005, Zhu *et al.* 2007, Bakhti *et al.* 2013, Barzoki *et al.* 2015, Bidgoli *et al.* 2015, Tagrara *et al.* 2015). Ashrafi and Hubert (Ashrafi and Hubert 2006) modeled the elastic properties of CNTRCs through a finite element analysis. Xu *et al.* (Xu *et al.* 2006) examined the thermal behavior of SWCNT polymer-matrix composites. Han and Elliott (Han and Elliott 2007) used molecular dynamics (MD), to simulate the elastic properties of CNTRCs. These studies proved that adding a small amount of carbon nanotube can significantly improve the mechanical, electrical, and thermal properties of polymeric composites. Studies on CNTRCs have also revealed that distributing CNTs in a uniform way as the reinforcements in the matrix can give only intermediate improvement of the mechanical characteristics (Qian *et al.* 2000, Seidel and Lagoudas 2006). This is principally because of the weak interfacial bonding strength between the CNTs and matrix. Shen (Shen 2009) extended the idea of FGMs to CNTRCs and founded out that a graded distribution of CNTs in the matrix can lead to an interfacial bonding strength. Ke *et al.* (Ke *et al.* 2010, Ke *et al.* 2013) examined the effect of FG-CNT volume fraction on the nonlinear vibration and dynamic stability of composite beams. Wang and Shen (Wang and Shen 2011) studied the vibration of CNTRC plates in thermal environments. They mentioned that the CNTRC plates with symmetrical distribution of CNTs have lower natural frequencies, but lower linear to nonlinear frequency ratios than ones with unsymmetrical or uniform distribution of CNTs. Wang and Shen (Wang and Shen 2012) studied the nonlinear bending and vibration of sandwich plates with CNTRC face sheets in sandwich structures with FG-CNTRC face

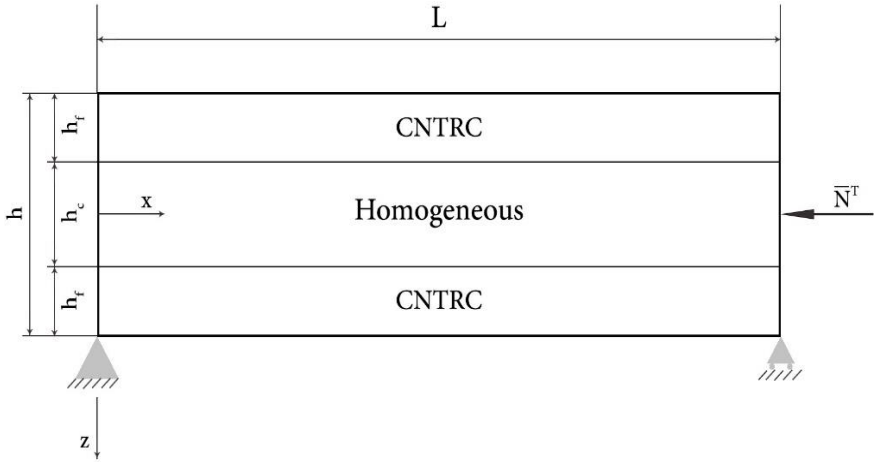

Fig. 1 A simple scheme of sandwich beam with CNTRC face sheets

sheets. The effects of nanotube volume fraction, foundation stiffness, core-to-facing thickness ratio, temperature change, and in-plane boundary conditions on the nonlinear vibration and bending behaviors of sandwich plates with CNTRC facings sheets were considered. Yang *et al.* (Yang *et al.* 2015) examined the dynamic buckling FG nanocomposite beams reinforced by CNT as a core and integrated with two surface bonded piezoelectric layers. Wu *et al.* (Wu *et al.* 2015) investigated free vibration and buckling behavior of sandwich beams reinforced with FG-CNTRCs face sheets based on Timoshenko beam theory but they considered neither the temperature dependency of the material properties nor the thermal environment effects on the structure.

In this paper thermo-mechanical vibration of sandwich beams with a stiff core and FG-CNTRC face sheets reinforced by SWCNTs are investigated within the framework of Timoshenko beam theory. The material characteristic of carbon nanotubes are supposed to change in the thickness direction in a functionally graded form. DTM is employed to solve the differential governing equations of sandwich beams. A parametric study is conducted to investigate the effects of carbon nanotube volume fraction, slenderness ratio, core-to-face sheet thickness ratio, different thermal environment and various boundary conditions on the free vibration characteristics of FG-CNTRC sandwich beams.

2. CNTRC sandwich beam

Consider a symmetric sandwich beam with the length of L, width b and total thickness h subjected to an axial load caused by thermal expansion. As shown in Fig. 1 the sandwich beam is made of two CNTRC face sheets with thickness of h_f and a stiff core layer of thickness h_c. Three different types of support conditions namely, simply supported-simply supported (S-S), clamped-clamped (C-C) and clamped-simply supported (C-S) are considered individually. Moreover two distributions of CNTs, i.e., *V*-graded and uniform distributions, are considered.

The material properties can be determined from the rule of mixture as

$$E_{11} = \eta_1 V_{cn} E_{11}^{cn} + V_m E_m \tag{1a}$$

$$\frac{\eta_2}{E_{22}} = \frac{V_{cn}^*}{E_{22}^{cn}} + \frac{V_m}{E_{22}^m} \tag{1b}$$

$$\frac{\eta_3}{G_{12}} = \frac{V_{cn}^*}{G_{12}^{cn}} + \frac{V_m}{G_m} \tag{1c}$$

where E_{11}^{cn}, E_{22}^{cn} and G_{12}^{cn} are Young's moduli and shear modulus of CNTs, respectively. E_m and G_m are the properties for the matrix. $\eta_i(i=1,2,3)$ is CNT efficiency parameter accounting for the scale-dependent material properties and can be obtained by matching the elastic modulus of CNTRCs achieved from molecule dynamic simulation and those which are extracted from rule of mixture. V_m and V_{cn} are the volume fraction of matrix and the CNTs, respectively. The relation between them can be expressed as

$$V_{cn} + V_m = 1 \tag{2}$$

It is supposed that for the FG-CNTRC face sheets V_{cn} changes linearly across the thickness the top face sheet as follows

$$V_{cn} = \frac{-(2z + h_c)}{h_f} V_{cn}^* \tag{3a}$$

and also for the bottom face sheet

$$V_{cn} = \frac{(2z - h_c)}{h_f} V_{cn}^* \tag{3b}$$

in which V^* can be described as

$$V_{cn}^* = \frac{w_{cn}}{w_{cn} + \frac{\rho_{cn}}{\rho_m} - \frac{\rho_{cn}}{\rho_m} w_{cn}} \tag{4}$$

where w_{cn} is the mass fraction of CNT, and ρ_m and ρ_{cn} are the densities of matrix and CNT, respectively. There is a simple relation for V^*_{cn} in UD-CNTRCs which can be given by: $V_{cn}=V^*_{cn}$, so it's obvious that the mass fraction for UD-CNTRC and FG-CNTRC face sheets are equal. The density and Poisson's ratio of the CNTRC face sheets can be described in order as

$$\nu = V_{cn}\nu_{cn} + V_m\nu_m \tag{5}$$

$$\rho = V_{cn}\rho_{cn} + V_m\rho_m \tag{6}$$

in which v_m and v_{cn} are Poisson's ratio of the matrix and CNT, respectively. Because functionally graded structures, such as sandwich beams in this case, are used mostly in high temperature environment, eventually significant changes in mechanical properties of the ingredient materials are to be expected, it is necessary to take into account this temperature-dependency for precise prediction of the mechanical reaction. Thus, Young's modulus and thermal expansion coefficient

Table 1 Temperature dependent properties of Young's modulus and thermal expansion coefficient for Ti-6A1-4V

Material	Properties	P_0	P_{-1}	P_1	P_2	P_3
Ti-6Al-4V	$E\,(Pa)$	122.56e+9	0	-4.586e-4	0	0
	$\alpha(K^{-1})$	7.5788e-6	0	6.638e-4	-3.147e-6	0

Table 2 Temperature dependent properties of Young's modulus and thermal expansion coefficient for CNTs

Temperature (°*K*)	${E_{11}}^{cn}(Tpa)$	${E_{22}}^{cn}(Tpa)$	${G_{12}}^{cn}(Tpa)$	$\alpha^{cn}(K^{-1})$
300	5.6466	7.0800	1.9445	3.4584
500	5.5308	6.9348	1.9643	4.5361
700	5.4744	6.8641	1.9644	4.6677

believed to be functions of temperature, as to be shown in Section 3.1, so that E and α are both temperature and position dependent. The behavior of FG materials can be predicted under high temperature more precisely with considering the temperature dependency on material properties. The nonlinear equation of thermo-elastic material properties in function of temperature $T(K)$ can be expressed as (Shen 2004)

$$P = P_0(P_{-1}T^{-1} + 1 + P_1T + P_2T^2 + P_3T^3) \tag{7}$$

where P_0, P_{-1}, P_1, P_2 and P_3 are the temperature dependent coefficients which are presented in Table 1. For composite host, PMMA matrix has been chosen. Eventually there are different expressions to describe the temperature dependent properties of PMMA; $\alpha^m=45(1+0.0005\Delta T)\times 10^{-6}/K$, $E^m=(3.52-0.0034T)Gpa$, in which $T=T_0+\Delta T$ and $T_0=300K$ (Yang *et al.* 2015). To predict the correct CNT properties which is dependent to temperature (Zhang and Shen 2006), we should estimate CNT efficiency parameters η_1 and η_2 by matching the Young's modulus E_{11} and E_{22} of CNTRCs obtained by the rule of mixture to those obtained from the MD simulations given by Han and Elliott (Han and Elliott 2007). It should be noted that only E_{11} should be used in beam theories. The results are shown in Table 2.

3. Theoretical formulations

3.1 Governing equations

The displacement of an arbitrary point in the beam along the x and z directions, according to Timoshenko beam theory can be expressed by

$$\overline{U}(x,z,t) = U(x,t) + z\,\psi(x,t), \quad \overline{W}(x,z,t) = W(x,t), \tag{8}$$

where $U(x,t)$ and $W(x,t)$ are displacement elements of a point in the mid-plane, t is time and ψ is the rotation of the beam cross-section. The linear strain-displacement relationship can be described as

$$\varepsilon_{xx} = \frac{\partial U}{\partial x} + z\,\frac{\partial \psi}{\partial x}, \quad \gamma_{xz} = \frac{\partial W}{\partial x} + \psi. \tag{9}$$

The normal stress and shear stress are expressed as

$$\sigma_{xx} = Q_{11}(z)\left(\frac{\partial U}{\partial x} + z\,\frac{\partial \psi}{\partial x}\right), \quad \sigma_{xz} = Q_{55}(z)\left(\frac{\partial W}{\partial x} + \psi\right), \tag{10}$$

where

$$Q_{11}(z) = \frac{E(z)}{1-\nu^2}, \quad Q_{55}(z) = \frac{E(z)}{2(1+\nu)}. \tag{11}$$

The normal force, bending moment and transverse shear force resultants are presented as

$$N_x = \int_{-h/2}^{h/2} \sigma_{xx}\,dz = A_{11}\frac{\partial U}{\partial x} + B_{11}\frac{\partial \psi}{\partial x}, \tag{12a}$$

$$M_x = \int_{-h/2}^{h/2} \sigma_{xx}\,z\,dz = B_{11}\frac{\partial U}{\partial x} + D_{11}\frac{\partial \psi}{\partial x}, \tag{12b}$$

$$Q_x = \kappa\int_{-h/2}^{h/2} \sigma_{xz}\,dz = \kappa\left(A_{55}\frac{\partial W}{\partial x} + \psi\right), \tag{12c}$$

where the shear correction factor is expressed by κ=5/6. The inertia related terms and stiffness components can be determined from

$$\{I_1, I_2, I_3\} = \int_{-h/2}^{h/2} \rho(z)\{1, z, z^2\}dz \tag{13a}$$

$$\{A_{11}, B_{11}, D_{11}\} = \int_{-h/2}^{h/2} Q_{11}(z)\{1, z, z^2\}dz \quad , \quad A_{55} = \int_{-h/2}^{h/2} Q_{55}(z)dz \tag{13b}$$

The governing equations of motion of the beam, by using Hamilton's principle can be defined as

$$\frac{\partial N_x}{\partial x} = I_1\frac{\partial^2 U}{\partial t^2} + I_2\frac{\partial^2 \psi}{\partial t^2}, \tag{14a}$$

$$\frac{\partial Q_x}{\partial x} + \overline{N}^T\frac{\partial^2 W}{\partial x^2} = I_1\frac{\partial^2 W}{\partial t^2}, \tag{14b}$$

$$\frac{\partial M_x}{\partial x} - Q_x = I_2\frac{\partial^2 U}{\partial t^2} + I_3\frac{\partial^2 \psi}{\partial t^2}. \tag{14c}$$

in which coefficient K_s is called the Timoshenko shear correction factor and its exact value depends on the material properties and cross section parameters of the beam. Here, K_s for rectangular beams has been assumed to be 5/6. Also $\overline{N}^T$ is the thermal resultant and can be described as

$$\bar{N}^T = \int_{-h/2}^{h/2} E\left(z,T\right)\alpha\left(z,T\right)\left(T-T_0\right)dz \tag{15}$$

where T_0 is the reference temperature. For simply supported-simply supported (S-S), clamped-clamped (C-C) and clamped-simply supported (C-S) sandwich beams with a movable end at $x=L$, the boundary conditions require

$$U=0,\ W=0,\ M_x=0,\quad \text{at } x=0, \tag{16a}$$

$$N_x=0,\ W=0,\ M_x=0,\quad \text{at } x=L, \tag{16b}$$

for a S-S beam,

$$U=0,\ W=0,\ \psi=0,\quad \text{at } x=0, \tag{17a}$$

$$N_x=0,\ W=0,\ \psi=0,\quad \text{at } x=L, \tag{17b}$$

for a C-C beam and

$$U=0,\ W=0,\ M_x=0,\quad \text{at } x=0, \tag{18a}$$

$$N_x=0,\ W=0,\ \psi=0,\quad \text{at } x=L, \tag{18b}$$

for a C-S beam.

3.2 Dimensionless governing equations

It is better first to clarify the following dimensionless quantities

$$\begin{gathered}\xi=\frac{x}{L},\ (u,w)=\frac{(U,W)}{h},\ N^T=\frac{\bar{N}^T}{A_{110}},\ \left(\bar{I}_1,\bar{I}_2,\bar{I}_3\right)=\left(\frac{I_1}{I_{10}},\frac{I_2}{I_{10}h},\frac{I_3}{I_{10}h^2}\right),\\ \varphi=\psi,\ \lambda=\frac{L}{h},\ \left(a_{11},a_{55},b_{11},d_{11}\right)=\left(\frac{A_{11}}{A_{110}},\kappa\frac{A_{55}}{A_{110}},\frac{B_{11}}{A_{110}h},\frac{D_{11}}{A_{110}h^2}\right),\\ \tau=\frac{t}{L}\sqrt{\frac{A_{110}}{I_{10}}},\ \omega=\Omega L\sqrt{\frac{I_{10}}{A_{110}}},\end{gathered} \tag{19}$$

where I_{10} and A_{110} are the values of I_1 and A_{11} of a homogeneous beam made from pure core material. Dimensionless natural frequency of the sandwich beam is expressed by ω. With respect to Eq. (18), and substituting Eq. (12) into Eq. (14), the final equations can then be explained in dimensionless form as

$$a_{11}\frac{\partial^2 u}{\partial\zeta^2}+b_{11}\frac{\partial^2\varphi}{\partial\zeta^2}=\bar{I}_1\frac{\partial^2 u}{\partial\tau^2}+\bar{I}_2\frac{\partial^2\varphi}{\partial\tau^2}, \tag{20a}$$

$$a_{55}\left(\frac{\partial^2 w}{\partial\zeta^2}+\lambda\frac{\partial\varphi}{\partial\zeta}\right)-N^T\frac{\partial^2 w}{\partial\zeta^2}=\bar{I}_1\frac{\partial^2 w}{\partial\tau^2}, \tag{20b}$$

$$b_{11}\frac{\partial^2 u}{\partial \zeta^2}+d_{11}\frac{\partial^2 \varphi}{\partial \zeta^2}-a_{55}\lambda\left(\frac{\partial w}{\partial \zeta}+\lambda\varphi\right)=\bar{I}_2\frac{\partial^2 u}{\partial \tau^2}+\bar{I}_3\frac{\partial^2 \varphi}{\partial \tau^2}, \tag{20c}$$

then the transformed boundary conditions turn into

$$u=0,\ w=0,\ \phi=0,\quad \text{at } \zeta=0, \tag{21a}$$

$$a_{11}\frac{\partial u}{\partial \zeta}+b_{11}\frac{\partial \varphi}{\partial \zeta},\ w=0,\ \phi=0,\quad \text{at } \zeta=L, \tag{22b}$$

for a S-S sandwich beam

$$u=0,\ w=0,\ b_{11}\frac{\partial u}{\partial \zeta}+d_{11}\frac{\partial \varphi}{\partial \zeta}=0,\quad \text{at } \zeta=0, \tag{22a}$$

$$a_{11}\frac{\partial u}{\partial \zeta}+b_{11}\frac{\partial \varphi}{\partial \zeta},\ w=0,\ b_{11}\frac{\partial u}{\partial \zeta}+d_{11}\frac{\partial \varphi}{\partial \zeta}=0,\quad \text{at } \zeta=L, \tag{22b}$$

for a C-C sandwich beam and

$$u=0,\ w=0,\ \phi=0,\quad \text{at } \zeta=0, \tag{23a}$$

$$a_{11}\frac{\partial u}{\partial \zeta}+b_{11}\frac{\partial \varphi}{\partial \zeta},\ w=0,\ b_{11}\frac{\partial u}{\partial \zeta}+d_{11}\frac{\partial \varphi}{\partial \zeta}=0,\quad \text{at } \zeta=L, \tag{23b}$$

for a C-S sandwich beam.

4. Uniform temperature rise (UTR)

The initial temperature of the sandwich beam is assumed to be (T_0=300K), which is a stress free state and is uniformly changed to the final temperature of T. The temperature rise is given by

$$\Delta T\ =T\ -T_0 \tag{24}$$

5. Solution procedure

5.1 Application of differential transform method to free vibration problem

Differential transform method (DTM) is a semi-analytic transformation technique based on Taylor series expansion equations and is a useful tool to obtain analytical solutions of differential equations. Certain transformations rules are applied to governing equations and the boundary conditions of the system in order to transform them into a set of algebraic equations in terms of the differential transforms of the original functions. This method construct an analytical solution in the form of polynomials. It is different from the high-order Taylor series method, which requires

Table 3 Some transformation rules for one-dimensional DTM (Ju 2004)

Original function	Transformed function
$f(x)=g(x)\pm h(x)$	$F(K)=G(K)\pm H(K)$
$f(x)=\lambda g(x)$	$F(K)=\lambda G(K)$
$f(x)=g(x)h(x)$	$F(K)=\sum_{l=0}^{K} G(K-l)H(l)$
$f(x)=\frac{d^n g(x)}{dx^n}$	$F(K)=\frac{(k+n)!}{k!}G(K+n)$
$f(x)=x^n$	$F(K)=\delta(K-n)=\begin{cases}1 & k=n\\ 0 & k\neq n\end{cases}$

symbolic computation of the necessary derivative of the data functions and is expensive for large orders. The Taylor series method is computationally expansive for large orders. Differential transformation of the n^{th} derivative of the function $y(x)$ and differential inverse transformation of $Y(k)$ are respectively defined as (Hassan 2002)

$$Y(k)=\frac{1}{k!}\left[\frac{d^k}{dx^k}y(x)\right]_{x=0} \tag{25}$$

$$y(x)=\sum_{k=0}^{\infty} x^k Y(k) \tag{26}$$

in which $y(x)$ is the original function and $Y(k)$ is the transformed function. As a consequently of Eqs. (25), (26) the following relation can be obtained

$$y(x)=\sum_{k=0}^{\infty}\frac{x^k}{k!}\left[\frac{d^k}{dx^k}y(x)\right]_{x=0} \tag{27}$$

$$y(x)=\sum_{k=0}^{n} x^k Y(k) \tag{28}$$

In this calculations $y(x)=\sum_{k=n+1}^{\infty} x^k Y(k)$ is small enough to be neglected, and n is determined by the convergence of the eigenvalues. From definitions of DTM in Eqs. (47)-(49), the fundamental theorems of differential transforms method can be performed which are listed in Table 4. While Table 4 presents the differential transformation of conventional boundary conditions. First we assume the following variation for $w(x,t)$ and $\theta(x,t)$

$$w(x,t)=\bar{w}e^{i\omega t} \text{ and } \theta(x,t)=\bar{\theta}e^{i\omega t} \tag{29}$$

by reducing u and substituting Eq. (29) into Eq. (20), the equations of motions may be turned to

$$a_{55}\left(\frac{\partial^2 w}{\partial\zeta^2}+\lambda\frac{\partial\phi}{\partial\zeta}\right)-N_{x0}\frac{\partial^2 w}{\partial\zeta^2}=-I_1\omega^2 w(\zeta) \tag{30}$$

$$-\frac{b_{11}^{\ 2}}{a_{11}}\frac{\partial^2\varphi}{\partial\zeta^2}+d_{11}\frac{\partial^2\varphi}{\partial\zeta^2}-a_{55}\lambda\left(\frac{\partial w}{\partial\zeta}+\lambda\varphi\right)=\bar{I}_2\omega^2\frac{b_{11}}{a_{11}}\varphi-\bar{I}_3\omega^2\varphi \tag{31}$$

According to the basic transformation operations presented in Table 3, the transformed form of the governing Eqs. (30) and (31) around x_0=0 may be obtained as

$$a_{55}\left[(k+1)(k+2)W(k+2)+\lambda(k+1)\phi(k+1)\right]-N_x(k+1)(k+2)W(k+2)=-I_1\omega^2W(k) \tag{32}$$

$$\left(d_{11}-\frac{b_{11}^{\ 2}}{a_{11}}\right)(k+1)(k+2)\phi(k+2)-a_{55}\lambda\left[(k+1)W(k+1)+\lambda\phi\right]=-\omega^2\left(\bar{I}_3\phi-\bar{I}_2\frac{b_{11}}{a_{11}}\phi\right) \tag{33}$$

Also by using the theorems introduced in Table 4, various transformed boundary conditions can be expressed as follows:

• Simply supported-Simply supported

$$w[0]=0,\ \varphi[1]=0$$

$$\sum_{k=0}^{\infty}w[k]=0,\ \sum_{k=0}^{\infty}k\ \varphi[k]=0 \tag{34a}$$

• Clamped-Simply supported

$$w[0]=0,\ \varphi[0]=0$$

$$\sum_{k=0}^{\infty}w[k]=0,\ \sum_{k=0}^{\infty}k\ \varphi[k]=0 \tag{34b}$$

• Clamped-Clamped

$$w[0]=0,\ \varphi[0]=0$$

$$\sum_{k=0}^{\infty}w[k]=0,\ \sum_{k=0}^{\infty}\varphi[k]=0 \tag{34c}$$

Now by using Eqs. (32) and (33) together with the transformed boundary conditions one can obtain the following eigenvalue problem

$$\begin{bmatrix} M_{11}^{(n)}(\omega) & M_{12}^{(n)}(\omega) \\ M_{21}^{(n)}(\omega)_{21} & M_{22}^{(n)}(\omega) \end{bmatrix}[C]=0 \tag{35}$$

where [C] corresponds to the missing boundary conditions at x=0 and $M_{ij}^{(n)}$ are the polynomials in terms of (ω) corresponding to the *nth* term. For the non-trivial solutions of Eq. (35), it is necessary that the determinant of the coefficient matrix set equal to zero

Table 4 Transformed boundary conditions based on DTM (Ju 2004)

x=0		x=L	
Original B.C.	Transformed B.C.	Original B.C.	Transformed B.C.
$f(0)=0$	$F[0]=0$	$f(L)=0$	$\sum_{k=0}^{\infty}F[k]=0$
$\frac{df(0)}{dx}=0$	$F[1]=0$	$\frac{df(L)}{dx}=0$	$\sum_{k=0}^{\infty}k\,F[k]=0$
$\frac{d^2f(0)}{dx^2}=0$	$F[2]=0$	$\frac{d^2f(L)}{dx^2}=0$	$\sum_{k=0}^{\infty}k(k-1)F[k]=0$
$\frac{d^3f(0)}{dx^3}=0$	$F[3]=0$	$\frac{d^3f(L)}{dx^3}=0$	$\sum_{k=0}^{\infty}k(k-1)(k-2)F[k]=0$

Table 5 Convergence study for the first three frequencies with FG-CNTRC face sheets (L/h=20, h_c/h_f=8)

n	ω_1	ω_2	ω_3
12	0.14499	-	-
13	0.14502	-	-
14	0.14503	-	-
15	0.14504	0.54167	-
16	0.14504	0.59675	0.72903
17	0.14504	0.58092	0.83827
18	0.14504	0.57080	42.7243
19	0.14504	0.57184	5.0476
20	0.14504	0.57289	1.05913
21	0.14504	0.57279	1.11939
22	0.14504	0.57269	41.59312
23	0.14504	0.57270	6.07850
24	0.14504	0.57270	1.23659
25	0.14504	0.57270	1.24982
26	0.14504	0.57270	1.26681
27	0.14504	0.57270	1.26417
28	0.14504	0.57270	1.26180
29	0.14504	0.57270	1.26206
30	0.14504	0.57270	1.26232
31	0.14504	0.57270	1.26227
32	0.14504	0.57270	1.26227
33	0.14504	0.57270	1.26227

$$\begin{bmatrix} M_{11}^{(n)}(\omega) & M_{12}^{(n)}(\omega) \\ M_{21}^{(n)}(\omega)_{21} & M_{22}^{(n)}(\omega) \end{bmatrix}=0 \tag{36}$$

Table 6 Comparison of first three dimensionless natural frequencies of S-S sandwich beams with FG-CNTRC face sheets (L/h=20, h_c/h_f=8)

Mode		V^*_{cn}=0.12		V^*_{cn}=0.17		V^*_{cn}=0.28	
		Present	(Wu *et al.* 2015)	Present	(Wu *et al.* 2015)	Present	(Wu *et al.* 2015)
1	FG	0.1450	0.1453	0.1594	0.1588	0.1844	0.1825
	UD	0.1429	0.1432	0.1566	0.1560	0.1806	0.1785
2	FG	0.5727	`0.5730	0.6289	0.6247	0.7261	0.7174
	UD	0.5643	0.5650	0.6180	0.6140	0.7114	0.6997
3	FG	1.2623	1.2599	1.3837	1.3689	1.5933	1.5554
	UD	1.2444	1.2429	1.3605	1.3465	1.5623	1.5246

Table 7 First three dimensionless natural frequencies of C-C sandwich beams with FG-CNTRC face sheets (L/h=20, h_c/h_f=8)

Mode		V^*_{cn}=0.12		V^*_{cn}=0.17		V^*_{cn}=0.28	
		Present	(Wu *et al.* 2015)	Present	(Wu *et al.* 2015)	Present	(Wu *et al.* 2015)
1	FG	0.3239	0.3240	0.3528	0.3530	0.4031	0.4032
	UD	0.3192	0.3195	0.3467	0.3470	0.3950	0.3949
2	FG	0.8724	0.8704	0.9483	0.9443	1.0800	1.0699
	UD	0.8602	0.8588	0.9327	0.9291	1.0594	1.0492
3	FG	1.6626	1.6520	1.8026	1.7838	2.0441	2.0029
	UD	1.6404	1.6313	1.7744	1.7569	2.0086	1.9672

The *i th* estimated eigenvalue may be obtained by the *n th* iteration, by solving Eq. (36). The total number of iterations are related to the accuracy of calculations can be determined by the following equation

$$\left|\omega_i^{(n)} - \omega_i^{(n-1)}\right| < \varepsilon \tag{37}$$

6. Results and discussion

6.1 Comparison studies

Before starting to study the free vibration analysis of sandwich beams with CNTRC facing sheets, a comparison is made between the present results and those from the open literature in order to validate the present formulation. Table 5 shows the number of repetition for convergence of the first three frequencies using DTM. It is found that in DTM after a certain number of iterations eigenvalues converged to a value with good precision. According to Table 5 the first natural frequency converged after 15 iterations with 4 digit precision while the second and third ones converged after 23 and 31 iterations respectively. Table 6 compares numerical dimensionless natural frequency of the simply-supported FG sandwich beams with the analytical results (Wu *et al.* 2015). As it can be seen, the proposed results match very well with the results of reference paper. Moreover,

Table 8 Effect of nanotube volume fraction on first three natural frequencies of sandwich beams with FG-CNTRC face sheets (L/h=20, h_c/h_f=8)

			ΔT=0			ΔT=200			ΔT=400		
Mode	B.S.		V^*_{cn}			V^*_{cn}			V^*_{cn}		
			0.12	0.17	0.28	0.12	0.17	0.28	0.12	0.17	0.28
1	S-S	FG	0.1450	0.1595	0.1844	0.1393	0.1538	0.1789	0.1340	0.1487	0.1741
	S-S	UD	0.1429	0.1566	0.1806	0.1370	0.1509	0.1749	0.1317	0.1457	0.1699
2	S-S	FG	0.5727	0.6289	0.7261	0.5518	0.6086	0.7065	0.5319	0.5899	0.6893
	S-S	UD	0.5643	0.6180	0.7114	0.5432	0.5976	0.6917	0.5231	0.5785	0.6741
3	S-S	FG	1.2623	1.3837	1.5933	1.2166	1.3394	1.5505	1.1725	1.2980	1.5124
	S-S	UD	1.2444	1.3605	1.5623	1.1983	1.3159	1.5193	1.1539	1.2740	1.4807
1	C-C	FG	0.3239	0.3528	0.4031	0.3121	0.3414	0.3922	0.3008	0.3309	0.3826
	C-C	UD	0.3192	0.3467	0.3950	0.3072	0.3353	0.3841	0.2958	0.3245	0.3742
2	C-C	FG	0.8724	0.9483	1.0800	0.8407	0.9177	1.0508	0.8100	0.8891	1.0246
	C-C	UD	0.8602	0.9327	1.0594	0.8283	0.9019	1.0300	0.7973	0.8729	1.0034
3	C-C	FG	1.6626	1.8026	2.0441	1.6003	1.7425	1.9891	1.5423	1.6881	1.9379
	C-C	UD	1.6404	1.7744	2.0086	1.5778	1.7140	1.9505	1.5193	1.6579	1.8989
1	C-S	FG	0.2251	0.2474	0.2857	0.2167	0.2391	0.2778	0.2088	0.2316	0.2708
	C-S	UD	0.2218	0.2430	0.2799	0.2133	0.2347	0.2718	0.2052	0.2270	0.2647
2	C-S	FG	0.7166	0.7860	0.9059	0.6905	0.7607	0.8814	0.6655	0.7372	0.8597
	C-S	UD	0.7063	0.7727	0.8880	0.6801	0.7472	0.8634	0.6548	0.7234	0.8414
3	C-S	FG	1.4584	1.5962	1.8337	1.4052	1.5446	1.7838	1.3538	1.4961	1.7389
	C-S	UD	1.4383	1.5703	1.7992	1.3848	1.5184	1.7492	1.3329	1.4694	1.7039

the first three dimensionless natural frequencies for the C-C FG-CNTRC beam are tabulated in Table 7. The parameters used in this example are the same as those in Ref. (Wu *et al.* 2015). A good agreement is obtained, again.

6.2 Free vibration analysis

In this study, poly (methyl methacrylate), i.e., PMMA with E_m=2.5 Gpa, ρ_m=1190 kg/m^3 and ν_m=0.3, is choosen to be the matrix material for CNTRCs. The armchair (10, 10) SWCNTs, with material properties of E_{11}^{cn}=5.6466 TPa, E_{22}^{cn}=7.08 TPa, G_{12}^{cn}=1.9445 TPa, ρ_{cn}=1400 kg/m^3 and ν_{cn}=0.175 at room temperature, (Shen and Zhang 2010) are selected as the reinforcement for CNTRCs. The CNT efficiency parameter η_j is obtained by matching the Young's modulus E_{11} and E_{22} and shear modulus G_{12} of CNTRCs determined from the rule of mixture against those from the MD simulations given by Han and Elliott (Han and Elliott 2007). The following values presented by Shen and Zhang (Shen and Zhang 2010): η_1=0.137, η_2=1.022, η_3=0.075 are used for the case of V^*_{cn}=0.12, η_1=0.142, η_2=1.626, η_3=1.138 for V^*_{cn}=0.17; and η_1=0.141, η_2=1.585, η_3=1.109 for V^*_{cn}=0.28. Also, Titanium alloy is chosen for. Titanium alloy (Ti-6Al-4V) as the core material has the following characteristics: E_c=113.8 GPa, ρ_c=4430 kg/m^3 and ν_c=0.342. The thickness of the sandwich beam is chosen as 10 mm totally, and kept unchanged in all numerical situations while the thickness of core layer and face sheets change arbitrarily as the core-to-face sheet thickness ratio

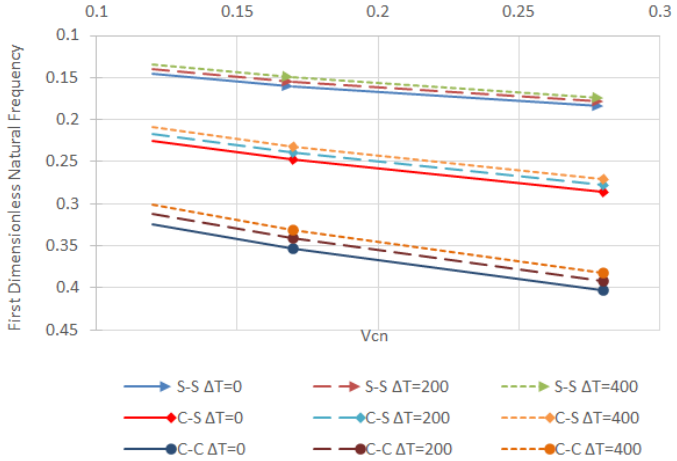

Fig. 2 First three dimensionless natural frequencies of C-C, S-S and C-S sandwich beams with CNTRC face sheets with different CNT volume fraction

Table 9 Dimensionless first three natural frequencies of sandwich beams with FG-CNTRC face sheets and different values of L/h(h_c/h_f=8, V^*_{cn}=0.17)

			ΔT=0			ΔT=200			ΔT=400		
Mode	B.S.		L/h			L/h			L/h		
			10	20	30	10	20	30	10	20	30
1	S-S	FG	0.3145	0.1595	0.1066	0.3043	0.1538	0.1021	0.2945	0.1487	0.0983
	S-S	UD	0.3090	0.1566	0.1047	0.2988	0.1509	0.1001	0.2893	0.1457	0.0962
2	S-S	FG	1.1943	0.6289	0.4237	1.1556	0.6086	0.4094	1.1192	0.5899	0.3965
	S-S	UD	1.1752	0.6180	0.4162	1.1363	0.5976	0.4018	1.0995	0.5785	0.3886
3	S-S	FG	2.4953	1.3837	0.9434	2.4116	1.3394	0.9130	2.3315	1.2980	0.8849
	S-S	UD	2.4597	1.3605	0.9270	2.3757	1.3159	0.8964	2.2952	1.2740	0.8678
1	C-C	FG	0.6661	0.3528	0.2379	0.6443	0.3414	0.2300	0.6237	0.3309	0.2227
	C-C	UD	0.6557	0.3467	0.2337	0.6339	0.3353	0.2257	0.6131	0.3245	0.2183
2	C-C	FG	1.6884	0.9483	0.6483	1.6308	0.9177	0.6272	1.5753	0.8891	0.6078
	C-C	UD	1.6657	0.9327	0.6371	1.6078	0.9019	0.6159	1.5521	0.8729	0.5962
3	C-C	FG	3.0220	1.8026	1.2518	2.9148	1.7425	1.2115	2.8114	1.6881	1.1747
	C-C	UD	2.9874	1.7744	1.2308	2.8794	1.7140	1.1902	2.7758	1.6579	1.1529
1	C-S	FG	0.4781	0.2474	0.1660	0.4626	0.2391	0.1599	0.4482	0.2316	0.1547
	C-S	UD	0.4702	0.2430	0.1630	0.4547	0.2347	0.1596	0.4400	0.2270	0.1515
2	C-S	FG	1.4468	0.7860	0.5331	1.3987	0.7607	0.5156	1.3529	0.7372	0.4995
	C-S	UD	1.4254	0.7727	0.5238	1.3772	0.7472	0.5061	1.3311	0.7234	0.4898
3	C-S	FG	2.7758	1.5962	1.0983	2.6799	1.5446	1.0629	2.5874	1.4961	1.0301
	C-S	UD	2.7397	1.5703	1.0795	2.6438	1.5184	1.0439	2.5510	1.4694	1.0107

is changed with the following values: h_c/h_f=8, 6, 4. The natural frequencies with respect to the effect of initial thermal environment are presented in Tables 8-10. Table 8 and Fig. 2 present the

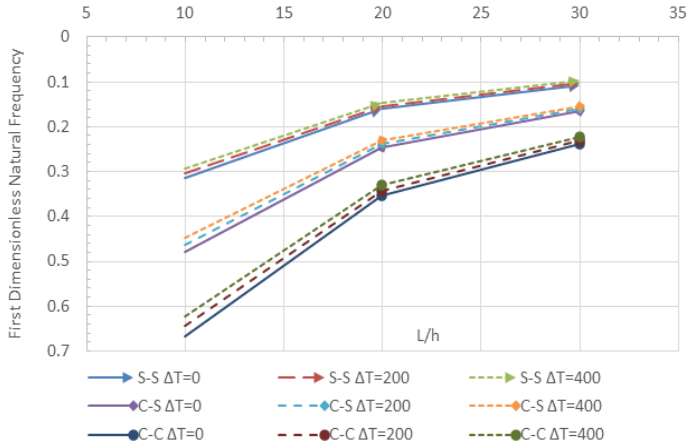

Fig. 3 First three natural frequencies of C-C, S-S and C-S sandwich beams with CNTRC face sheets with different slenderness ratios

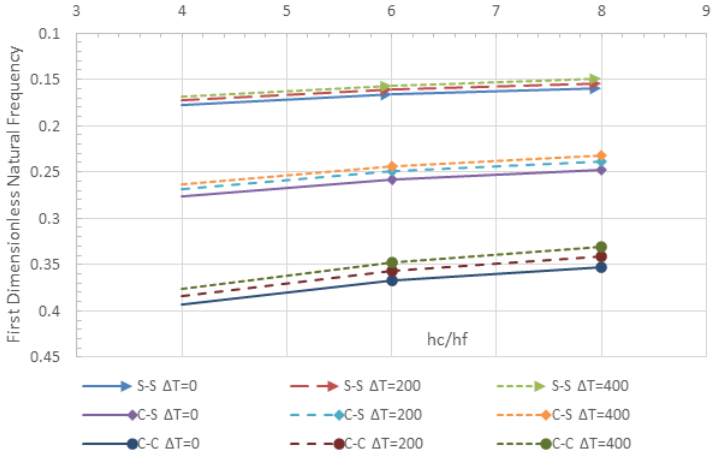

Fig. 4 First three natural frequencies of C-C, S-S and C-S sandwich beams with CNTRC face sheets with different core-to-face thickness ratio

first three natural frequencies of C-C, S-S and C-S sandwich beams with CNTRC face sheets with different CNT volume fractions V^*_{cn}.

The core-to-face sheet thickness ratio and the slenderness ratio are kept unchanged at h_c/h_f=8 and L/h=20, respectively. It is observed that the natural frequency of the sandwich beam increases with an increase in the CNT volume fraction V^*_{cn} but decreases as the temperature increases. The C-C sandwich beam has a higher natural frequency than the same C-S beam and the C-S beam higher than S-S one. Furthermore, it is observed that the natural frequencies of the sandwich beam with UD-CNTRC face sheets is also lower than those of the beam with FG-CNTRC face sheets. This is because the sandwich beam with UD-CNTRC face sheets has a lower stiffness than the beam with FG-CNTRC face sheets.

Table 9 and Fig. 3 present the first three natural frequencies of C-C, S-S and C-S sandwich beams with CNTRC face sheets but with different slenderness ratio L/h. The core-to-face sheet thickness ratio and the CNT volume fraction are kept unchanged at h_c/h_f=8 and V^*_{cn}=0.17,

Table 10 Dimensionless first three natural frequencies of sandwich beams with FG-CNTRC face sheets and various values of h_c/h_f (L/h=20, V^*_{cn}=0.17)

			ΔT=0			ΔT=200			ΔT=400		
Mode	B.S.		h_c/h_f			h_c/h_f			h_c/h_f		
			8	6	4	8	6	4	8	6	4
1	S-S	FG	0.1595	0.1661	0.1779	0.1538	0.1607	0.1729	0.1487	0.1560	0.1686
	S-S	UD	0.1566	0.1617	0.1703	0.1509	0.1562	0.1651	0.1457	0.1513	0.1606
2	S-S	FG	0.6289	0.6549	0.7016	0.6086	0.6362	0.6849	0.5899	0.6194	0.6708
	S-S	UD	0.6180	0.6380	0.6721	0.5976	0.6191	0.6553	0.5785	0.6020	0.6408
3	S-S	FG	1.3837	1.4406	1.5427	1.3394	1.3998	1.5065	1.2980	1.3629	1.4756
	S-S	UD	1.3605	1.4047	1.4803	1.3159	1.3636	1.4440	1.2740	1.3262	1.4126
1	C-C	FG	0.3528	0.3673	0.3934	0.3414	0.3568	0.3840	0.3309	0.3474	0.3760
	C-C	UD	0.3467	0.3579	0.3770	0.3353	0.3473	0.3675	0.3245	0.3377	0.3594
2	C-C	FG	0.9483	0.9870	1.0564	0.9177	0.9587	1.0313	0.8891	0.9331	1.0097
	C-C	UD	0.9327	0.9628	1.0143	0.9019	0.9344	0.9892	0.8729	0.9084	0.9673
3	C-C	FG	1.8026	1.8741	2.0047	1.7425	1.8210	1.9575	1.6881	1.7710	1.9152
	C-C	UD	1.7744	1.8304	1.9290	1.7140	1.7772	1.8819	1.6579	1.7268	1.8394
1	C-S	FG	0.2474	0.2575	0.2759	0.2391	0.2499	0.2689	0.2316	0.2431	0.2631
	C-S	UD	0.2430	0.2508	0.2642	0.2347	0.2431	0.2572	0.2270	0.2361	0.2511
2	C-S	FG	0.7860	0.8183	0.8762	0.7607	0.7949	0.8555	0.7372	0.7740	0.8379
	C-S	UD	0.7727	0.7976	0.8404	0.7472	0.7741	0.8195	0.7234	0.7528	0.8015
3	C-S	FG	1.5962	1.6613	1.7781	1.5446	1.6136	1.7357	1.4961	1.5703	1.6992
	C-S	UD	1.5703	1.6212	1.7085	1.5184	1.5733	1.6661	1.4694	1.5295	1.6292

respectively. It is observed that the natural frequency of the sandwich beam decreases with an increase in the slenderness ratio but decreases as the temperature increases. The C-C sandwich beam has a higher natural frequency than the same C-S beam and the C-S beam higher than S-S one. Furthermore, it is observed that the natural frequencies of the sandwich beam with UD-CNTRC face sheets is also lower than that of the beam with FG-CNTRC face sheets. This is because the sandwich beam with UD-CNTRC face sheets has a lower stiffness than the beam with FG-CNTRC face sheets.

Table 10 and Fig. 4, present the first three natural frequencies of C-C, S-S and C-S sandwich beams with CNTRC face sheets but with different core-to-face thickness ratio h_c/h_f. The slenderness ratio and the CNT volume fraction are kept unchanged at L/h=20 and V^*_{cn}=0.17, respectively. It is observed that the natural frequency of the sandwich beam increases with an increase in the core-to-face thickness ratio but decreases as the temperature increases. The C-C sandwich beam has a higher natural frequency than the same C-S beam and the C-S beam higher than S-S one. Furthermore, it is observed that the natural frequencies of the sandwich beam with UD-CNTRC face sheets is also lower than that of the beam with FG-CNTRC face sheets. This is because the sandwich beam with UD-CNTRC face sheets has a lower stiffness than the beam with FG-CNTRC face sheets.

7. Conclusions

Thermo-mechanical vibration characteristics of sandwich beams with CNTRC face sheets have been examined based on the Timoshenko beam theory and semi analytical DTM. The effects of CNT volume fraction, core-to-face sheet thickness ratio, slenderness ratio, and end supporting conditions on the free vibration behaviors of stiff-cored sandwich beams with CNTRC face sheets with respect to uniform temperature change revealed through a parametric study. Numerical results show that CNT volume fraction, end supporting conditions, and slenderness ratio have a significant influence on the natural frequencies, whereas the effects of temperature change and core-to-face sheet thickness ratio is much less pronounced. The natural frequencies of the sandwich beam decrease with an increase in temperature change, core-to-face and slenderness ratio, but they increase with an increase in CNT volume fraction. The numerical results also point out that the sandwich beam with UD-CNTRC face sheets has lower vibration performances than FG-CNTRC the beam with face sheets.

References

Ajayan, P.O., Stephan, C.C. and Trauth, D. (1994), "Aligned carbon nanotube arrays formed by cutting a polymer resin-nanotube composite", *Sci*. **265**(5176), 1212-1214.

Anandrao, K.S., Gupta, R., Ramchandran, P. and Rao, G.V. (2010), "Thermal post-buckling analysis of uniform slender functionally graded material beams", *Struct*. *Eng*. *Mech*., **36**(5), 545-560.

Ashrafi, B. and Hubert, P. (2006), "Modeling the elastic properties of carbon nanotube array/polymer composites", *Compos*. *Sci*. *Technol*., **66**(3), 387-396.

Barzoki, A.A.M., Loghman, A. and Arani, A.G. (2015), "Temperature-dependent nonlocal nonlinear buckling analysis of functionally graded SWCNT-reinforced microplates embedded in an orthotropic elastomeric medium", *Struct*. *Eng*. *Mech*., **53**(3), 497-517.

Bhangale, R.K. and Ganesan, N. (2006), "Thermoelastic buckling and vibration behavior of a functionally graded sandwich beam with constrained viscoelastic core", *J*. *Sound Vibr*., **295**(1-2), 294-316.

Bidgoli, M.R., Karimi, M.S. and Arani, A.G. (2015), "Viscous fluid induced vibration and instability of FG-CNT-reinforced cylindrical shells integrated with piezoelectric layers", *Steel Compos*. *Struct*., **19**(3), 713-733.

Bonnet, P., Sireude, D., Garnier, B. and Chauvet, O. (2007), "Thermal properties and percolation in carbon nanotube-polymer composites", *Appl*. *Phys*. *Lett*., **91**(20), 201910-201910-201913.

Ebrahimi, F. and Rastgoo, A. (2008a) "Free vibration analysis of smart annular FGM plates integrated with piezoelectric layers", *Smart Mater*. *Struct*. **17**(1), 015044.

Ebrahimi, F. and Rastgoo, A. (2008b), "An analytical study on the free vibration of smart circular thin FGM plate based on classical plate theory", *Thin-Wall*. *Struct*., **46**(12), 1402-1408.

Ebrahimi, F. and Rastgoo, A. (2008c), "Free vibration analysis of smart FGM plates", *J*. *Mech*. *Syst*. *Sci*. *Eng*., **2**(2), 94-99.

Ebrahimi, F., Rastgoo, A. and Kargarnovin, M.H. (2008), "Analytical investigation on axisymmetric free vibrations of moderately thick circular functionally graded plate integrated with piezoelectric layers", *J*. *Mech*. *Sci*. *Technol*., **22**(6), 1058-1072.

Ebrahimi F., Rastgoo, A. and Atai, A.A. (2009a), "Theoretical analysis of smart moderately thick shear deformable annular functionally graded plate", *Eur*. *J*. *Mech*.-*A*/*Sol*., **28**(5), 962-997.

Ebrahimi, F., Naei, M.H. and Rastgoo, A. (2009b), "Geometrically nonlinear vibration analysis of piezoelectrically actuated FGM plate with an initial large deformation", *J*. *Mech*. *Sci*. *Technol*., **23**(8), 2107-2124.

Ebrahimi, F. (2013), "Analytical investigation on vibrations and dynamic response of functionally graded plate integrated with piezoelectric layers in thermal environment", *Mech*. *Adv*. *Mater*. *Struct*., **20**(10), 854-870.

Ebrahimi, F., Ghasemi, F. and Salari, E. (2016a), "Investigating thermal effects on vibration behavior of temperature-dependent compositionally graded euler beams with porosities", *Meccan*., **51**(1), 223-249.
Ebrahimi, F. and Zia, M. (2015), "Large amplitude nonlinear vibration analysis of functionally graded Timoshenko beams with porosities", *Acta Astronaut.*, **116**, 117-125.
Ebrahimi, F. and Mokhtari, M. (2015), "Transverse vibration analysis of rotating porous beam with functionally graded microstructure using the differential transform method", *J. Brazil. Soc. Mech. Sci. Eng*., **37**(4), 1435-1444.
Ebrahimi, F. and Salari, E (2015a), "Size-dependent thermo-electrical buckling analysis of functionally graded piezoelectric nanobeams", *Smart Mater. Struct*., **24**(12), 125007.
Ebrahimi, F. and Salari, E. (2015b), "Nonlocal thermo-mechanical vibration analysis of functionally graded nanobeams in thermal environment", *Acta Astronaut.*, **113**, 29-50.
Ebrahimi, F. and Salari, E. (2015c), "Size-dependent free flexural vibrational behavior of functionally graded nanobeams using semi-analytical differential transform method", *Compos. B*, **79**, 156-169.
Ebrahimi, F. and Salari, E. (2015d), "A semi-analytical method for vibrational and buckling analysis of functionally graded nanobeams considering the physical neutral axis position", *CMES*: *Comput. Model. Eng. Sci*., **105**(2), 151-181.
Ebrahimi, F. and Salari, E. (2015e), "Thermal buckling and free vibration analysis of size dependent Timoshenko FG nanobeams in thermal environments", *Compos. Struct.*, **128**, 363-380.
Ebrahimi, F. and Salari, E. (2015f), "Thermo-mechanical vibration analysis of nonlocal temperature-dependent FG nanobeams with various boundary conditions", *Compos. B*, **78**, 272-290.
Ebrahimi, F. and Salari, E. (2016), "Effect of various thermal loadings on buckling and vibrational characteristics of nonlocal temperature-dependent functionally graded nanobeams", *Mech. Adv. Mater. Struct*., **23**(12), 1379-1397.
Ebrahimi, F., Salari, E. and Hosseini, S.A.H. (2015), "Thermomechanical vibration behavior of FG nanobeams subjected to linear and non-linear temperature distributions", *J. Therm. Stress*., **38**(12), 1360-1386.
Ebrahimi, F., Salari, E. and Hosseini, S.A.H. (2016c), "In-plane thermal loading effects on vibrational characteristics of functionally graded nanobeams", *Meccan*., **51**(4), 951-977.
Ebrahimi, F. and Barati, M.R. (2016a), "Magneto-electro-elastic buckling analysis of nonlocal curved nanobeams", *Eur. Phys. J. Plus*, **131**(9), 346.
Ebrahimi, F. and Barati, M.R. (2016b), "Static stability analysis of smart magneto-electro-elastic heterogeneous nanoplates embedded in an elastic medium based on a four-variable refined plate theory", *Smart Mater. Struct*., **25**(10), 105014.
Ebrahimi, F. and Barati, M.R. (2016c), "Temperature distribution effects on buckling behavior of smart heterogeneous nanosize plates based on nonlocal four-variable refined plate theory", *J. Smart Nano Mater*., 1-25.
Ebrahimi, F. and Barati, M.R. (2016d), "An exact solution for buckling analysis of embedded piezoelectro-magnetically actuated nanoscale beams", *Adv. Nano Res*., **4**(2), 65-84.
Ebrahimi, F. and Barati, M.R. (2016e), "Buckling analysis of smart size-dependent higher order magneto-electro-thermo-elastic functionally graded nanosize beams", *J. Mech*., 1-11.
Ebrahimi, F. and Barati, M.R. (2016f), "A nonlocal higher-order shear deformation beam theory for vibration analysis of size-dependent functionally graded nanobeams", *Arab. J. Sci. Eng*., **41**(5), 1679-1690.
Ebrahimi, F. and Hosseini, S.H.S. (2016a), "Double nanoplate-based NEMS under hydrostatic and electrostatic actuations", *Eur. Phys. J. Plus*, **131**(5), 1-19.
Ebrahimi, F. and Hosseini, S.H.S. (2016b), "Nonlinear electroelastic vibration analysis of NEMS consisting of double-viscoelastic nanoplates", *Appl. Phys. A*, **122**(10), 922.
Ebrahimi, F. and Hosseini, S.H.S. (2016c), "Thermal effects on nonlinear vibration behavior of viscoelastic nanosize plates", *J. Therm. Stress*., **39**(5), 606-625.
Ebrahimi, F. and Nasirzadeh, P. (2015), "A nonlocal Timoshenko beam theory for vibration analysis of thick nanobeams using differential transform method", *J. Theoret. Appl. Mech*., **53**(4), 1041-1052.

Ebrahimi, F., Barati, M.R. and Haghi, P. (2017), "Thermal effects on wave propagation characteristics of rotating strain gradient temperature-dependent functionally graded nanoscale beams", *J. Therm. Stress.*, **40**(5), 535-547.
Ebrahimi, F. and Barati, M.R. (2016g), "Vibration analysis of smart piezoelectrically actuated nanobeams subjected to magneto-electrical field in thermal environment", *J. Vibr. Contr.*, 1077546316646239.
Ebrahimi, F. and Barati, M.R. (2016h), "Buckling analysis of nonlocal third-order shear deformable functionally graded piezoelectric nanobeams embedded in elastic medium", *J. Brazil. Soc. Mech. Sci. Eng.*, 1-16.
Ebrahimi, F. and Barati, M.R. (2016i), "Small scale effects on hygro-thermo-mechanical vibration of temperature dependent nonhomogeneous nanoscale beams", *Mech. Adv. Mater. Struct.*, In press.
Ebrahimi, F. and Barati, M.R. (2016j), "Dynamic modeling of a thermo-piezo-electrically actuated nanosize beam subjected to a magnetic field", *Appl. Phys. A*, **122**(4), 1-18.
Ebrahimi, F. and Barati, M.R. (2016k), "Magnetic field effects on buckling behavior of smart size-dependent graded nanoscale beams", *Eur. Phys. J. Plus*, **131**(7), 1-14.
Ebrahimi, F. and Barati, M.R. (2016l), "Vibration analysis of nonlocal beams made of functionally graded material in thermal environment", *Eur. Phys. J. Plus*, **131**(8), 279.
Ebrahimi, F. and Barati, M.R. (2016m), "A nonlocal higher-order refined magneto-electro-viscoelastic beam model for dynamic analysis of smart nanostructures", *J. Eng. Sci.*, **107**, 183-196.
Ebrahimi, F. and Barati, M.R. (2016n), "Small-scale effects on hygro-thermo-mechanical vibration of temperature-dependent nonhomogeneous nanoscale beams", *Mech. Adv. Mater. Struct.*, 1-13.
Ebrahimi, F. and Barati, M.R. (2016o), "A unified formulation for dynamic analysis of nonlocal heterogeneous nanobeams in hygro-thermal environment", *Appl. Phys. A*, **122**(9), 792.
Ebrahimi, F. and Barati, M.R. (2016p), "Electromechanical buckling behavior of smart piezoelectrically actuated higher-order size-dependent graded nanoscale beams in thermal environment", *J. Smart Nano Mater.*, **7**(2), 69-90.
Ebrahimi, F. and Barati, M.R. (2016q), "Wave propagation analysis of quasi-3D FG nanobeams in thermal environment based on nonlocal strain gradient theory", *Appl. Phys. A*, **122**(9), 843.
Ebrahimi, F. and Barati, M.R. (2016r), "Flexural wave propagation analysis of embedded S-FGM nanobeams under longitudinal magnetic field based on nonlocal strain gradient theory", *Arab. J. Sci. Eng.*, 1-12.
Ebrahimi, F. and Barati, M.R. (2016s), "On nonlocal characteristics of curved inhomogeneous Euler-Bernoulli nanobeams under different temperature distributions", *Appl. Phys. A*, **122**(10), 880.
Ebrahimi, F. and Barati, M.R. (2016t), "Buckling analysis of piezoelectrically actuated smart nanoscale plates subjected to magnetic field", *J. Intell. Mater. Syst. Struct.*, 1045389X16672569.
Ebrahimi, F. and Barati, M.R. (2016u), "Size-dependent thermal stability analysis of graded piezomagnetic nanoplates on elastic medium subjected to various thermal environments", *Appl. Phys. A*, **122**(10), 910.
Ebrahimi, F. and Barati, M.R. (2016v), "Magnetic field effects on dynamic behavior of inhomogeneous thermo-piezo-electrically actuated nanoplates", *J. Brazil. Soc. Mech. Sci. Eng.*, 1-21.
Ebrahimi, F. and Barati, M.R. (2017a), "Hygrothermal effects on vibration characteristics of viscoelastic FG nanobeams based on nonlocal strain gradient theory", *Compos. Struct.*, **159**, 433-444.
Ebrahimi, F. and Barati, M.R. (2017b), "A nonlocal strain gradient refined beam model for buckling analysis of size-dependent shear-deformable curved FG nanobeams", *Compos. Struct.*, **159**, 174-182.
Ebrahimi, F., Ehyaei, J. and Babaei, R. (2016), "Thermal buckling of FGM nanoplates subjected to linear and nonlinear varying loads on Pasternak foundation", *Adv. Mater. Res.*, **5**(4), 245-261.
Ebrahimi, F. and Jafari, A. (2016), "Buckling behavior of smart MEE-FG porous plate with various boundary conditions based on refined theory", *Adv. Mater. Res.*, **5**(4), 261-276.
Ebrahimi, F. and Barati, M.R. (2016), "An exact solution for buckling analysis of embedded piezoelectro-magnetically actuated nanoscale beams", *Adv. Nano Res.*, **4**(2), 65-84.
Ebrahimi, F. and Mohsen, D. (2007), "Dynamic modeling of embedded curved nanobeams incorporating surface effects", *Coupled Syst. Mech.*, **5**(3), 255-267.
Esawi, A.M. and Farag, M.M. (2007), "Carbon nanotube reinforced composites: potential and current

challenges", *Mater. Des.*, **28**(9), 2394-2401.
Fidelus, J., Wiesel, E., Gojny, F., Schulte, K. and Wagner, H. (2005), "Thermo-mechanical properties of randomly oriented carbon/epoxy nanocomposites", *Compos. Part A: Appl. Sci. Manufact.*, **36**(11), 1555-1561.
Griebel, M. and Hamaekers, J. (2004), "Molecular dynamics simulations of the elastic moduli of polymer-carbon nanotube composites", *Comput. Meth. Appl. Mech. Eng.*, **193**(17), 1773-1788.
Han, Y. and Elliott, J. (2007), "Molecular dynamics simulations of the elastic properties of polymer/carbon nanotube composites", *Comput. Mater. Sci.*, **39**(2), 315-323.
Hassan, I.A.H. (2002), "On solving some eigenvalue problems by using a differential transformation", *Appl. Math. Comput.*, **127**(1), 1-22.
Hu, N., Fukunaga, H., Lu, C., Kameyama, M. and Yan, B. (2005), "Prediction of elastic properties of carbon nanotube reinforced composites", *Proceedings of the Royal Society A: Mathematical, Physical and Engineering Science*, **461**(2058), 1685-1710.
Ju, S.P. (2004), "Application of differential transformation to transient advective-dispersive transport equation", *Appl. Math. Comput.*, **155**(1), 25-38.
Ke, L.L., Yang, J. and Kitipornchai, S. (2010), "Nonlinear free vibration of functionally graded carbon nanotube-reinforced composite beams", *Compos. Struct.*, **92**(3), 676-683.
Ke, L.L., Yang, J. and Kitipornchai, S. (2013), "Dynamic stability of functionally graded carbon nanotube-reinforced composite beams", *Mech. Adv. Mater. Struct.*, **20**(1), 28-37.
Lau, A.K.T. and Hui, D. (2002), "The revolutionary creation of new advanced materials-carbon nanotube composites", *Compos. Part B: Eng.*, **33**(4), 263-277.
Lau, K.T., Gu, C., Gao, G.H., Ling, H.Y. and Reid, S.R. (2004), "Stretching process of single-and multi-walled carbon nanotubes for nanocomposite applications", *Carb.*, **42**(2), 426-428.
Odegard, G., Gates, T., Wise, K., Park, C. and Siochi, E. (2003), "Constitutive modeling of nanotube–reinforced polymer composites", *Compos. Sci. Technol.*, **63**(11), 1671-1687.
Pradhan, S. and Murmu, T. (2009), "Thermo-mechanical vibration of FGM sandwich beam under variable elastic foundations using differential quadrature method", *J. Sound Vibr.*, **321**(1), 342-362.
Qian, D., Dickey, E.C., Andrews, R. and Rantell, T. (2000), "Load transfer and deformation mechanisms in carbon nanotube-polystyrene composites", *Appl. Phys. Lett.*, **76**(20), 2868-2870.
Rahmani, O. and Pedram, O. (2014), "Analysis and modeling the size effect on vibration of functionally graded nanobeams based on nonlocal Timoshenko beam theory", *J. Eng. Sci.*, **77**, 55-70.
Seidel, G.D. and Lagoudas, D.C. (2006), "Micromechanical analysis of the effective elastic properties of carbon nanotube reinforced composites", *Mech. Mater.*, **38**(8), 884-907.
Shen, H.S. (2004), "Thermal postbuckling behavior of functionally graded cylindrical shells with temperature-dependent properties", *J. Sol. Struct.*, **41**(7), 1961-1974.
Shen, H.S. (2009), "Nonlinear bending of functionally graded carbon nanotube-reinforced composite plates in thermal environments", *Compos. Struct.*, **91**(1), 9-19.
Shen, H.S. and Zhang, C.L. (2010), "Thermal buckling and postbuckling behavior of functionally graded carbon nanotube-reinforced composite plates", *Mater. Des.*, **31**(7), 3403-3411.
Thostenson, E.T. and Chou, T.W. (2003), "On the elastic properties of carbon nanotube-based composites: modelling and characterization", *J. Phys. D: Appl. Phys.* **36**(5), 573.
Tounsi, A., Houari, M.S.A. and Benyoucef, S. (2013), "A refined trigonometric shear deformation theory for thermoelastic bending of functionally graded sandwich plates", *Aerospace Sci.* Technol., **24**(1), 209-220.
Wang, Z.X. and Shen, H.S. (2011), "Nonlinear vibration of nanotube-reinforced composite plates in thermal environments", *Comput. Mater. Sci.*, **50**(8), 2319-2330.
Wang, Z.X. and Shen, H.S. (2012), "Nonlinear vibration and bending of sandwich plates with nanotube-reinforced composite face sheets", *Compos. Part B: Eng.*, **43**(2), 411-421.
Wu, H., Kitipornchai, S. and Yang, J. (2015), "Free vibration and buckling analysis of sandwich beams with functionally graded carbon nanotube-reinforced composite face sheets", *J. Struct. Stabil. Dyn.*, 1540011.
Xu, Y., Ray, G. and Abdel-Magid, B. (2006), "Thermal behavior of single-walled carbon nanotube polymer-matrix composites", *Compos. Part A: Appl. Sci. Manufact.*, **37**(1), 114-121.

Yang, J., Ke, L.L. and Feng, C. (2015), "Dynamic buckling of thermo-electro-mechanically loaded FG-CNTRC beams", *J. Struct. Stabil. Dyn.*, 1540017.

Zenkour, A. and Sobhy, M. (2010), "Thermal buckling of various types of FGM sandwich plates", *Compos. Struct.*, **93**(1), 93-102.

Zenkour, A.M. (2005), "A comprehensive analysis of functionally graded sandwich plates: Part 2-buckling and free vibration", *J. Sol. Struct.*, **42**(18-19), 5243-5258.

Zhang, C.L. and Shen, H.S. (2006), "Temperature-dependent elastic properties of single-walled carbon nanotubes: Prediction from molecular dynamics simulation", *Appl. Phys. Lett.*, **89**(8), 081904.

Zhu, R., Pan, E. and Roy, A. (2007), "Molecular dynamics study of the stress-strain behavior of carbon-nanotube reinforced Epon 862 composites", *Mater. Sci. Eng.: A.*, **447**(1), 51-57.

AI